

Energy bands and final-state effects in $K_{0.30}MoO_3$

G. K. Wertheim, L. F. Schneemeyer, and D. N. E. Buchanan
AT&T Bell Laboratories, Murray Hill, New Jersey 07974

(Received 18 March 1985; revised manuscript received 17 May 1985)

An x-ray photoemission spectroscopy study of the blue molybdenum bronze $K_{0.30}MoO_3$ shows a conduction band of Mo 4*d* character extending 2 eV below the Fermi level. The valence band lies between 2 and 10 eV. The Mo 3*d* core-electron spectrum has components at binding energies previously identified with Mo^{5+} and Mo^{6+} ions in related molybdenum oxide compounds. In this metallic system these two states are, however, of final-state origin, representing alternate screening channels and do not indicate that discrete valences are present in the initial state.

INTRODUCTION

The blue bronze $K_{0.30}MoO_3$ is an anisotropic metal^{1,2} that undergoes a charge-density-wave— (CDW) driven phase transition at 180 K.^{3–6} Below that temperature nonlinear current-voltage characteristics are observed when the applied electric field exceeds a small threshold field of the order of 100 mV/cm.⁷ This nonlinear dc conductivity is believed to be due to charge transport via a moving (“sliding”) CDW, a CDW which is depinned from the lattice and moves in a dc field. The study of $K_{0.30}MoO_3$ has resulted in the observation and better understanding of many interesting physical phenomena associated with sliding-CDW conductivity. These studies have shown analogies between the magnetic response of a spin glass and the transient electrical response of $K_{0.30}MoO_3$.⁸ They have given a description of the pinning of the CDW by a distribution of Debye oscillators.⁹ They have also provided proof that a frozen CDW metastable state can be produced at low temperatures.¹⁰

For $K_{0.30}MoO_3$ only qualitative information on the electronic structure, as deduced from optical reflectivity¹¹ and x-ray diffuse scattering studies,⁶ has been reported. However, fuller knowledge of the electronic structure is important for understanding the physical properties of this material. We have used x-ray photoemission spectroscopy (XPS) to examine the energy bands of this unusual material. According to crystallographic studies^{12,13} it consists of blocks of edge-sharing MoO_6 octahedra linked at corners into two-dimensional sheets. There are three types of octahedra which are distinguished by the number of edges which they share with their neighbors. Adjacent sheets are well separated and have no oxygen atoms in common. The potassium ions lie between these sheets. The resulting layer structure cleaves readily and has a strongly anisotropic conductivity in the plane of the layers.

EXPERIMENTAL

The single-crystal samples used in this study were prepared by electrolyzing fused-salt mixtures, as described by Wold *et al.*¹⁴ Powder x-ray diffraction confirmed the monoclinic $K_{0.30}MoO_3$ structure of the resulting materi-

als. The threshold field for non-Ohmic conduction was used as an indicator of chemical purity (see Ref. 2). Specimens, mounted with conducting epoxy cement, were cleaved in a vacuum of 10^{-9} Torr in a preparation chamber attached to a Hewlett-Packard 5950A ESCA spectrometer. They were introduced into the spectrometer without exposure to higher pressure. Spectra encompassing the valence and conduction bands and the Mo 3*d* and O 1*s* core levels were then recorded. Spectra of the potassium atoms are of lesser interest because the K^+ ions do not contribute to the conduction-band region. The potassium spectra are also more difficult to interpret because they contain significant contributions from interlayer atoms exposed by cleaving. All binding energies are referenced to the Fermi level of the compound, which was located at the cutoff in the conduction band. Wide scans, as well as C 1*s* spectra, were used to monitor surface contamination. Contamination buildup was slow enough so that a complete set of spectra could be recorded after each cleave.

RESULTS AND DISCUSSION

An x-ray photoemission spectrum of the valence-band region is shown in Fig. 1. The dominant feature, which lies between 2 and 10 eV, is the valence band. The weak feature between 2 eV and the Fermi level is the occupied part of the conduction band. The K 3*p* spin-orbit doublet lies just off scale at ~ 17 eV. The shape of the valence band is very similar to that reported for MoO_3 , and is characteristic of edge-sharing MoO_6 octahedra. Although the valence band is usually thought of as made up of oxygen 2*p* states, one expects substantial molybdenum 4*d* admixture by analogy with the related tungsten bronzes.¹⁵ Since the photoelectric cross section¹⁶ of the Mo 4*d* states at Al $K\alpha$ energy is 16 times greater than that of the O 2*p* states, the valence-band spectrum obtained by XPS is largely representative of the Mo 4*d* admixture into the valence band. The top of the band, where the O 2*p* character is strongest, may be significantly attenuated. The occupied conduction band, which lies between 2 eV and E_F should consist dominantly of Mo 4*d* states with only weak oxygen 2*p* admixture. It exhibits a resolution-

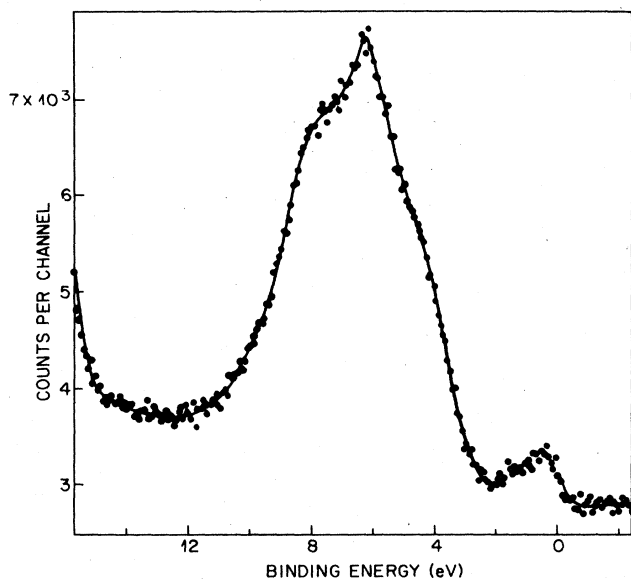


FIG. 1. X-ray photoemission spectrum of the valence-band region of $K_{0.30}MoO_3$.

limited cutoff at the Fermi energy in agreement with the metallic character of the material. The energy bands seen in Fig. 1 are in good accord with the molecular-orbital model presented in Ref. 11, but the gap between the valence and conduction bands is quite small. According to Ref. 11 the Mo $5s$ band should lie well above E_F .

The oxygen $1s$ core-electron spectrum shown in Fig. 2 has an asymmetric shape, but is cut off sharply at 533 eV

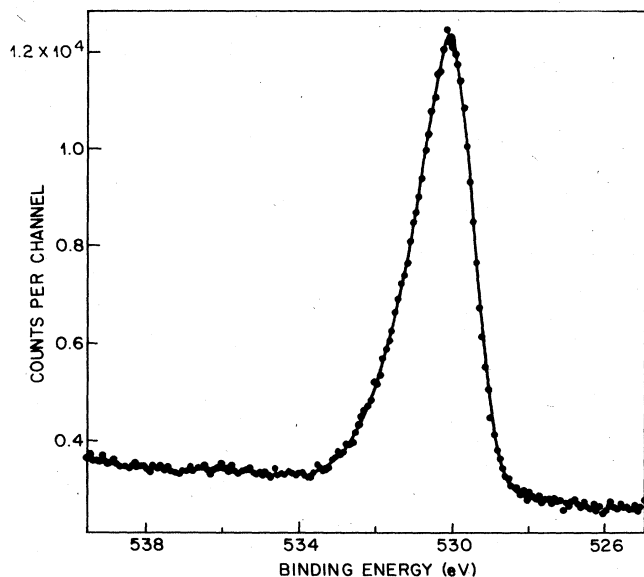


FIG. 2. Photoemission spectrum of the O $1s$ region of $K_{0.30}MoO_3$.

and is followed by a rising plasmon tail. It does not have the long, monotonically decaying tail produced by conduction-electron screening in metals.^{17,18} In the light of results obtained in other metallic oxides,¹⁹ in which it is found that only those atoms whose orbitals make up the conduction band are screened effectively by the conduction electrons, the lack of a many-body tail indicates that there is little O $2p$ character at the Fermi level. The asymmetric line shape is actually due to unresolved contributions from the many inequivalent oxygen sites in this crystal structure.^{12,13} Distinct oxygen core-electron binding energies are expected for atoms at corners shared by different numbers of octahedra, i.e., with different numbers of metal-atom neighbors. A spread in binding energies of ~ 1.5 eV is required to account for the width of the O $2p$ spectrum, but the individual contributions to the spectrum are difficult to isolate because the line has only two points of inflection.

A wide scan of the Mo $3d$ region shown in Fig. 3 shows a valence-band plasmon of 14 eV. The components of the $3d$ spin-orbit doublet are relatively broad compared to those found in MoO_3 , and give an indication of some poorly resolved structure. The $3d$ lines are shown on an expanded scale in Fig. 4. Although there are three inequivalent Mo sites in this structure we initially attempt to analyze the data into two components representing different valences, following the work of Refs. 20–22. As can be seen from the solid line through the data points in Fig. 4, two overlapping spin-orbit doublets, a broad symmetric one with $3d_{5/2}$ binding energy of 232.7 eV and a narrower asymmetric one at 231.5 eV, provide a fair approximation to the data. Components with similar bind-

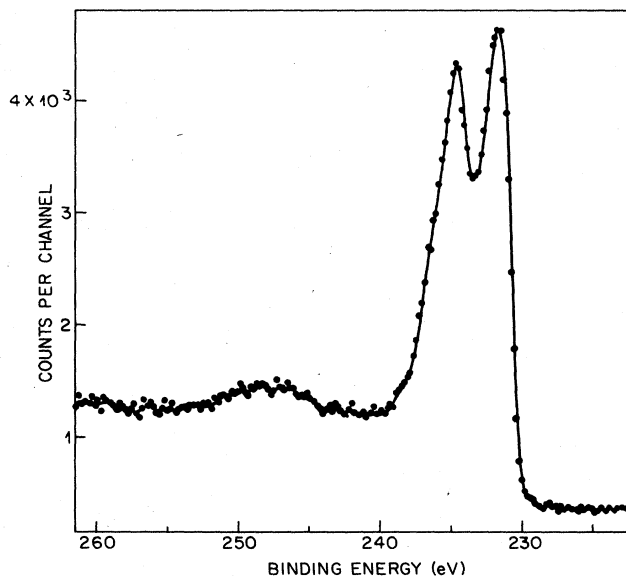


FIG. 3. Wide scan of the Mo $3d$ region of $K_{0.30}MoO_3$. The broad peak at 248 eV is due to excitation of a valence-band plasmon.

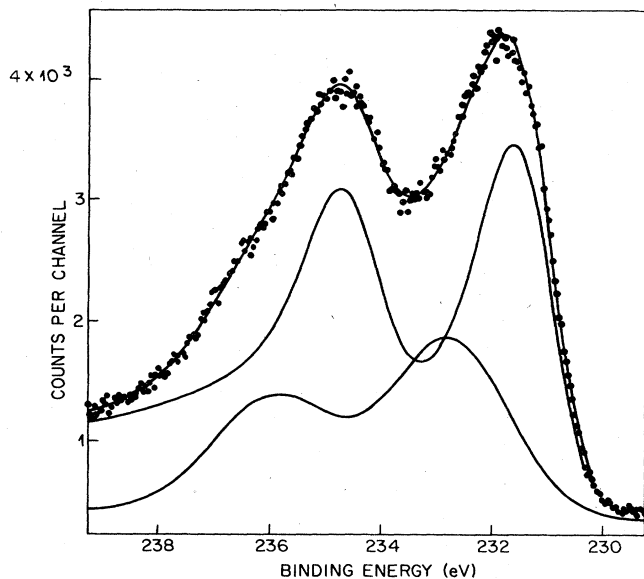


FIG. 4. The Mo $3d$ spectrum fitted with two spin-orbit doublets with common lifetime width and splitting, but independent singularity indexes and Gaussian widths. Note the misfit which is most apparent in the peak at 231.8 eV.

ing energies have been previously obtained for reduced MoO_3 and H_xMoO_3 .²⁰⁻²² The value of 232.7 eV agrees within the experimental error with that reported²² for stoichiometric MoO_3 , 232.6 eV, and is generally considered indicative of Mo^{6+} . The binding energy of the other line falls about halfway between that of MoO_3 and MoO_2 , 229.4 eV, motivating the assignment of lines at this energy to a $5+$ initial state.²¹

The agreement between Fermi-level-referenced binding energies in the insulating and metallic systems is the result of similarities in the band structures and final-state effects in these materials. Photoemission spectra show that the valence bands of materials made up of MoO_6 octahedra all have similar shapes and a similar binding energy relative to the Fermi level.²² In the insulators the conduction band lies just above the Fermi level; in the metallic systems it intersects the Fermi level. In insulating MoO_3 a core hole is screened by charge transfer from the valence band to the $4d$ conduction band. In $\text{K}_{0.30}\text{MoO}_3$ the same process may take place, resulting a final state with approximately the same energy. This is the higher-energy state identified as " $6+$ ". However, in a metallic system there is an alternate screening process, utilizing the electrons already in the d band, which produces a final state with lower energy. It is shifted by an amount equal to the excitation energy from the top of valence band to the Fermi level, and has a characteristic long-tailed, asymmetric line shape due to the collective response of the conduction electrons.¹⁷ The agreement between the excitation gap and the satellite energy in a variety of metallic transition-metal compounds indicates that these two screening channels are usually responsible for the two final states ob-

served in core-electron spectroscopy of these materials.²³

The applicability of the alternate point of view, which attributes the two components to valences present in the sample in the initial state, can be tested by the intensities of the two lines. In the present material, in which the potassium content is known with high accuracy, this initial-state interpretation leads to a significant difficulty, because the intensity of the $5+$ component is greater than that of the $6+$ component, while the expected intensity ratio is $3/7$. Surface effects, due to the loss of potassium from the cleaved surface, would enhance to $6+$ component and cannot account for the observations. In this connection it is worth noting that Tinetti *et al.*²¹ were unable to confirm the presence of Mo^{5+} in the EPR spectrum of H_xMoO_3 , another metallic system which yields XPS data with components at comparable binding energies. They attribute this discrepancy to a difference in the time scales of measurement in XPS and EPR. It is more accurate, however, to relate it to the final-state nature of XPS, i.e., to the fact that the XPS spectrum is determined not only by the initial state, but also by the response to the hole created by photoemission. The difference between EPR and XPS then lies in the difference between a measurement which gives exclusively initial-state information, and one which includes final-state effects. In the initial state no $5+$ ions are detected because the electrons in the $5d$ band are delocalized conduction electrons, not associated with a particular Mo atom.

It now remains to understand why the binding energy of the $5+$ state in the insulating systems is in agreement with that of the state screened by conduction electrons in a metallic system. In reduced, but still insulating, MoO_3 , electrons are trapped in the Mo $4d$ band near oxygen vacancies. When a Mo atom is core ionized, it may be screened by charge transfer as in MoO_3 , or else it may capture one of the electrons trapped in the $4d$ band, producing either of two distinct final states. One state is identical to that of MoO_3 , the other falls at smaller binding energy by an amount equal to the excitation energy from the top of the valence band to the Mo $4d$ band, just as in $\text{K}_{0.30}\text{MoO}_3$. The identification of this line as due to a Mo atom with $5+$ valence in the initial state is then made possible by the fact that the 2-eV excitation energy from the valence band to the Fermi level happens to be close to the 1.6-eV shift expected for a unit change in valence.

We now return to look more critically at the fit to the Mo $3d$ data in Fig. 4. The fit with two doublets is not entirely satisfactory. There are systematic deviations between the data and the fitted line at the peak of the lower-energy line. Similar deviations were found in the analysis of three independent data sets taken on different surfaces and with different scan widths, indicating that the model function with two doublets is not capable of reproducing the details of the data. Since the crystal structure contains three inequivalent Mo sites, each giving rise to two doublets, six doublets would be required to represent the full complexity of the situation. The data are, however, clearly not capable of defining that much detail. Since, according to Fig. 4, the three $6+$ components at greater binding energy could be adequately

represented by a single broad line, we left that part of the model function unchanged, but the component at smaller binding energy was broken up into its three constituents, yielding a four-doublet model. A fit with this model function did not converge because two of the sharp components tended to coincide. We consequently decided to reduce the number of component doublets to three, forcing two of them to coincide. The resulting fit, shown in Fig. 5, accounts much more satisfactorily for the shape of the low-energy peak, and yields a spectrum of residuals consisting entirely of the expected statistical fluctuations. This is the criterion by which we normally judge the success of a least-squares adjustment.

Additional support for this fit comes from the intensities of the two narrow components, which can be related to the occupancy of the three inequivalent sites in the $K_{0.30}MoO_3$ structure. The component at smallest binding energy, which has $\sim \frac{3}{5}$ of the intensity, is tentatively assigned to Mo atoms in octahedra sharing three and four edges, contain $\frac{2}{5}$ and $\frac{1}{5}$, respectively, of the molybdenum. The weaker component at larger binding energy is then due to the Mo atoms in octahedra which share only two edges, and contribute less strongly to the bottom of the conduction band. The other Mo atoms are believed to make the major contribution to the bottom of the conduction band because they have more Mo neighbors, resulting in a broader d band. Most of the charge donated by the K atoms into the Mo $4d$ band is then associated with these atoms which consequently have the smallest core-electron binding energies.

The solid line through the data points is the sum of the resulting three doublets and the plasmon-tail background. The doublets shown have a common spin-orbit splitting of 3.17 eV and a common spin-orbit ratio of 0.66, both

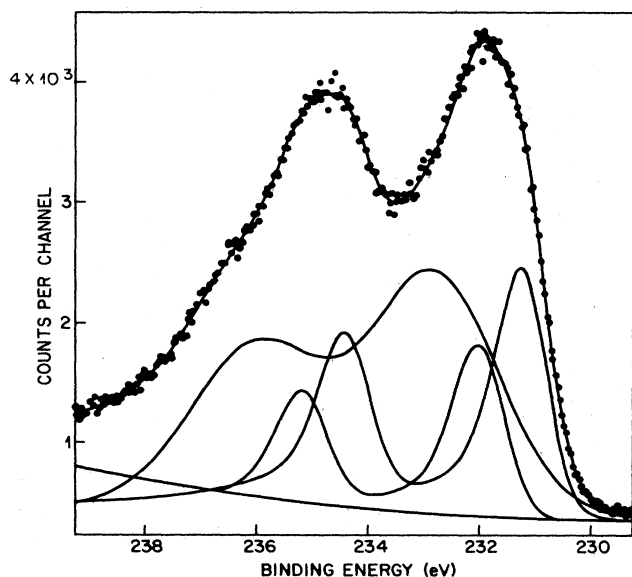


FIG. 5. The same data as in Fig. 4, but fitted with three spin-orbit doublets as described in the text.

determined by the least-squares adjustment. The two narrow components at smaller binding energy have the long-tailed, asymmetric line shape indicative of conduction-electron screening.^{17,18} The symmetric component, which falls close to the binding energy reported for MoO_3 , is broadened both by the unresolved contributions from the three inequivalent Mo sites, and by the excitation of phonons during photoemission. These results are quite similar to those obtained in the sodium tungsten bronzes which have a broad component close to the binding energy of WO_3 , and a narrow, asymmetrical one at a smaller binding energy.^{23,24}

The ratio of the sum of the areas of the two narrow components to that of the broad one in Fig. 5 is close to unity, i.e., still far from the composition-based value of $\frac{3}{7}$. This indicates that the intensities are determined not by the average valence of the initial state, but by the competition between metallic and charge-transfer screening.

A measure of the conduction-electron screening response is obtained from the asymmetry of the photoemission line. The tail toward greater binding energy is due to the excitation of electron-hole pairs, which have a spectral energy distribution given by $(\omega - \omega_0)^{\alpha-1}$, where α is the singularity index.¹⁷ The more effective the screening, the greater the value of α . The fit shown in Fig. 5 yields an α of 0.18, significantly smaller than that obtained for the W $4f$ lines of similar tungsten bronzes,²⁴ which typically have values greater than 0.3. Although the singularity index could not be determined with high precision because of the overlapping lines, it could nevertheless be shown that the data are not compatible with a value as large as that in the sodium tungsten bronzes. This may be an indication that the anisotropy of the conduction band of $K_{0.30}MoO_3$ limits the effectiveness of the screening response. It is not clear, however, whether the screening should be thought of as one or two dimensional. Based on optical reflectivity data, interpreted as showing a Drude edge typical of metals only when the electric field is polarized along the b axis,⁶ $K_{0.30}MoO_3$ has been called a one-dimensional conductor. However, higher-dimensional interactions are clearly of importance in this material, as they are in other materials with moving CDW's. All materials so far identified in which sliding CDW's are observed are anisotropic with a single high-conductivity axis. The large perturbation provided by the core hole probably allows a response by the entire layer.

CONCLUSIONS

These measurements have shown that the conduction band of $K_{0.30}MoO_3$ extends 2 eV below the Fermi level, and has largely Mo $4d$ character. The valence band is similar in shape and location to that of other compounds composed of MoO_6 octahedra. The band structure is largely in agreement with the model of Travaglini *et al.*,¹¹ but the gap between the valence and conduction bands is small. Core-electron spectra are dominated by final-state effects, and provide no information about

initial-state valences. Two final states, representing alternate screening channels, are identified. In the lowest energy state the Mo-core hole is screened by electrons in the Mo 4*d* conduction band, producing an asymmetric line.

In the higher-energy state the screening is by charge transfer, as it is in insulating MoO₃. This behavior is typical of metallic transition-metal compounds in which the top of the valence band lies close to the Fermi level.

-
- ¹R. Brusetti, B. K. Chakraverty, Y. Deveny, J. Dumas, J. Marcus, and C. Schlenker, *Recent Developments in Condensed Matter Physics*, edited by J. T. Devreese (Plenum, New York, 1981), Vol. 2, p. 181.
- ²L. F. Schneemeyer, F. J. DiSalvo, R. M. Fleming, and J. V. Waszczak, *J. Solid State Chem.* **54**, 358 (1984).
- ³M. Sato, H. Fujishita, and S. Hoshino, *J. Phys. C* **16**, L877 (1983).
- ⁴C. H. Chen, L. F. Schneemeyer, and R. M. Fleming, *Phys. Rev. B* **29**, 3765 (1984).
- ⁵R. M. Fleming, L. F. Schneemeyer, and D. E. Moncton, *Phys. Rev. B* **31**, 899 (1985).
- ⁶J. P. Pouget, S. Kagoshima, C. Schlenker, and J. Marcus, *J. Phys. (Paris) Lett.* **44**, L113 (1983).
- ⁷J. Dumas, C. Schlenker, J. Marcus, and R. Buder, *Phys. Rev. Lett.* **50**, 757 (1983).
- ⁸R. M. Fleming and L. F. Schneemeyer, *Phys. Rev. B* **28**, 6996 (1983).
- ⁹R. J. Cava, R. M. Fleming, P. Littlewood, E. A. Rietman, L. F. Schneemeyer, and R. G. Dunn, *Phys. Rev. B* **30**, 3228 (1984).
- ¹⁰R. J. Cava, R. M. Fleming, E. A. Rietman, R. G. Dunn, and L. F. Schneemeyer, *Phys. Rev. Lett.* **53**, 1677 (1984).
- ¹¹G. Travaglini, P. Wachter, J. Marcus, and C. Schlenker, *Solid State Commun.* **37**, 599 (1981).
- ¹²J. Graham and A. D. Wadsley, *Acta Crystallogr.* **20**, 93 (1966).
- ¹³M. Ghedira, J. Chenavas, M. Marezio, and J. Marcus (unpublished).
- ¹⁴A. Wold, W. Kunmann, R. J. Arnett, and A. Ferretti, *Inorg. Chem.* **3**, 545 (1964).
- ¹⁵L. F. Mattheiss, *Phys. Rev. B* **2**, 3918 (1970); **6**, 4718 (1972).
- ¹⁶J. H. Scofield, *J. Electron Spectrosc. Relat. Phenom.* **8**, 129 (1976).
- ¹⁷S. Doniach and M. Šunjić, *J. Phys. C* **3**, 385 (1970).
- ¹⁸G. K. Wertheim and S. Hüfner, *Phys. Rev. Lett.* **35**, 53 (1975).
- ¹⁹See, for example, the discussion of the Ba lines in BaBiO₃ by G. K. Wertheim, J. P. Remeika, and D. N. E. Buchanan, *Phys. Rev. B* **26**, 2120 (1982).
- ²⁰R. J. Colton, A. M. Guzman, and J. W. Rabalais, *Acc. Chem. Res.* **11**, 170 (1978).
- ²¹D. Tinetti, P. Canesson, H. Estrade, and J. J. Fripiat, *J. Phys. Chem. Solids* **41**, 583 (1979).
- ²²T. H. Fleisch and J. G. Mains, *J. Chem. Phys.* **76**, 780 (1982).
- ²³G. K. Wertheim, *X Ray and Inner Shell Processes in Atoms, Molecules and Solids*, edited by A. Meisel and J. Finster (Karl-Marx-Universität, Leipzig, 1984), p. 375.
- ²⁴J.-N. Chazalviel, M. Campagna, and G. K. Wertheim, *Phys. Rev. B* **16**, 697 (1977).